

# Fråga 12.1

- Vilket randvillkor gäller vid  $x=L_2$  om diffusionskonstanten är  $18 \text{ cm}^2/\text{s}$

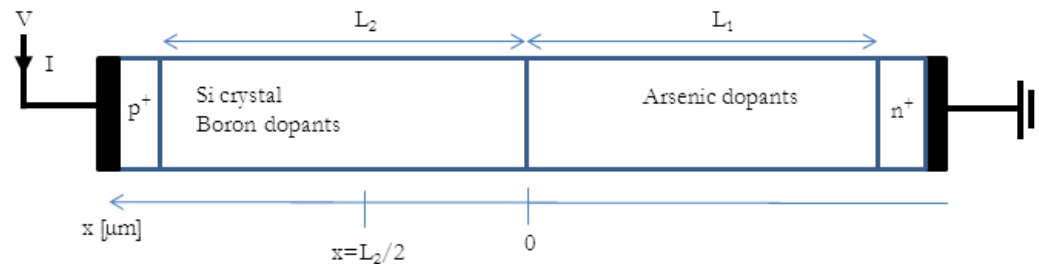
A)  $p'(x=L_2)=0$

B)  $p'(x=\infty)=0$

C)  $n'(x=L_2)=0$

D)  $n'(x=\infty)=0$

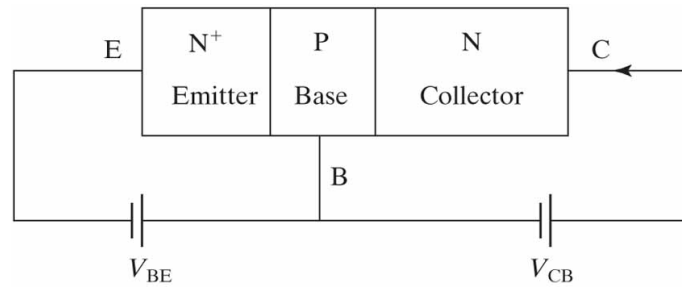
2. Calculate the electron concentration at  $x=L_2/2$  on the p-side of the pn junction below when  $V=24kT/q$ . The boron concentration is  $10^{17} \text{ cm}^{-3}$  and the arsenic concentration is  $10^{20} \text{ cm}^{-3}$ . The carrier lifetime is  $100 \mu\text{s}$  between  $x=0$  and  $x=L_2=10 \mu\text{m}$ .



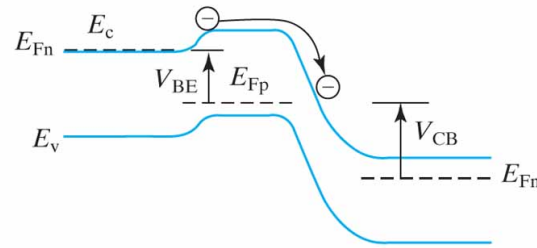
## Fråga 12.2

- Vad är sant för en struktur med n-p-n dopning. När går en stor ström från första n- till andra n-området?
    - A) Om det första n-området ansluts till positiv potential och det andra till negativ.
    - B) Om det första n-området ansluts till negativ potential och det andra till positiv.
    - C) Om p-området ansluts till positiv potential och det andra n-området till negativ.
    - D) Om p-området ansluts till positiv potential och det andra n-området till positiv.
-

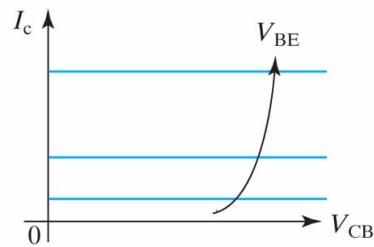
**Figure 8.1** (a) Schematic NPN BJT and normal voltage polarities; (b) electron injection from emitter into base produces and determines  $I_C$ ; and (c)  $I_C$  is basically determined by  $V_{BE}$  and is insensitive to  $V_{CB}$ .



(a)



(b)



(c)

**Figure 8.2** (a) Common-emitter convention; (b)  $I_C$  vs.  $V_{CE}$ ; (c)  $I_B$  may be used as the parameter instead of  $V_{BE}$ ; and (d) circuit symbol of an NPN BJT and an inverter circuit.

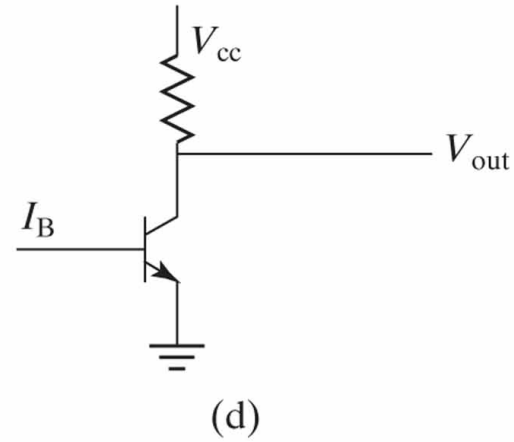
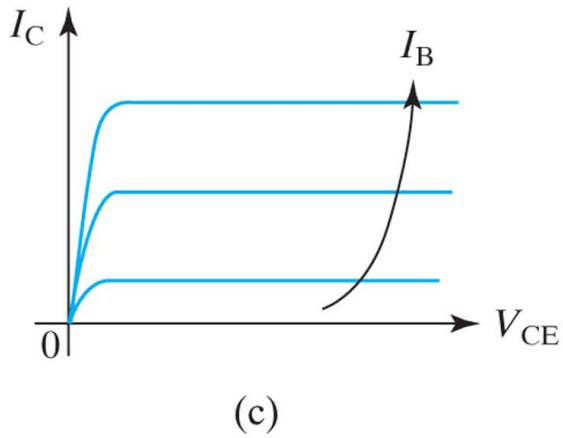
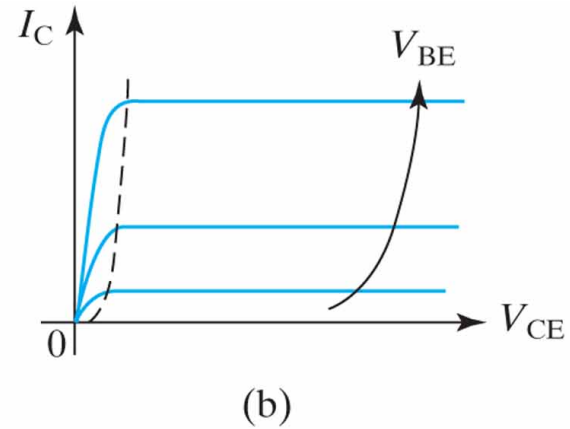
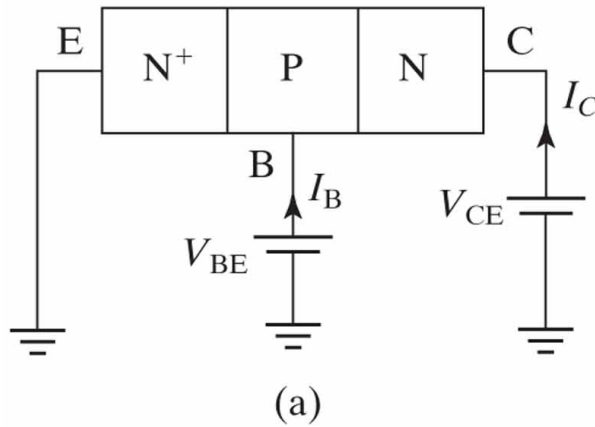


**Figure 8.3**  $x = 0$  is the edge of the BE junction depletion layer.  $W_B$  is the width of the base neutral region.

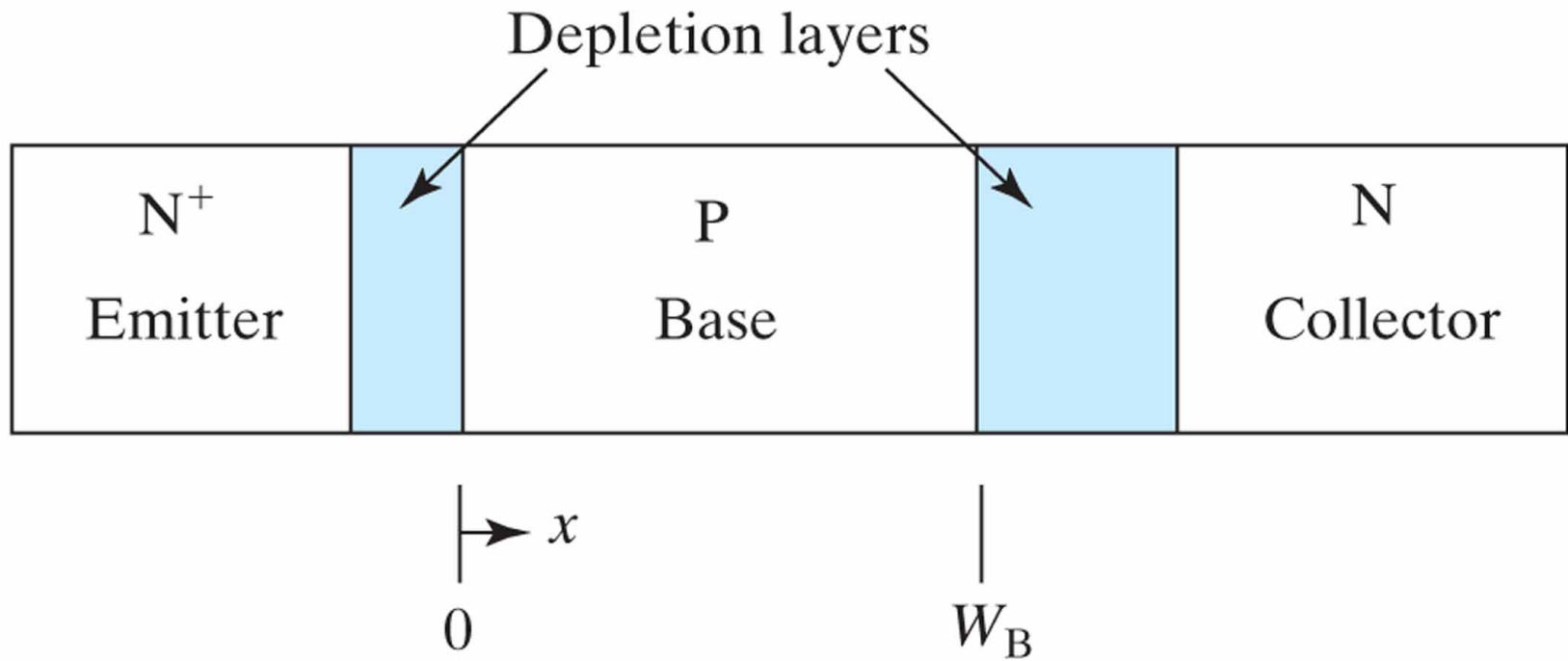


**Figure 8.4** When  $W_B \ll L_B$ , the excess minority carrier concentration in the base is approximately a linear function of  $x$ .

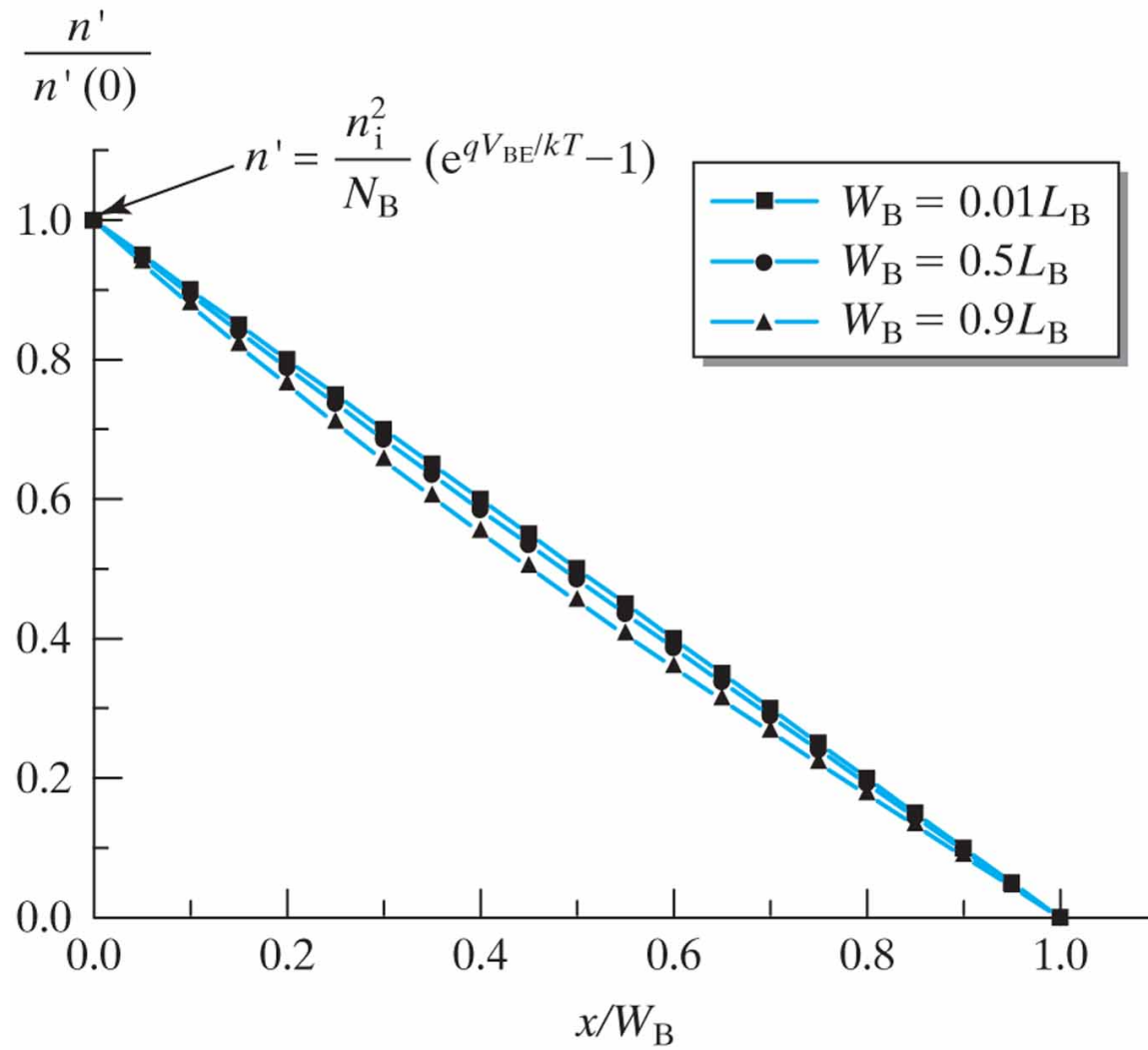


**Figure 8.5**  $I_C$  is an exponential function of  $V_{BE}$ .

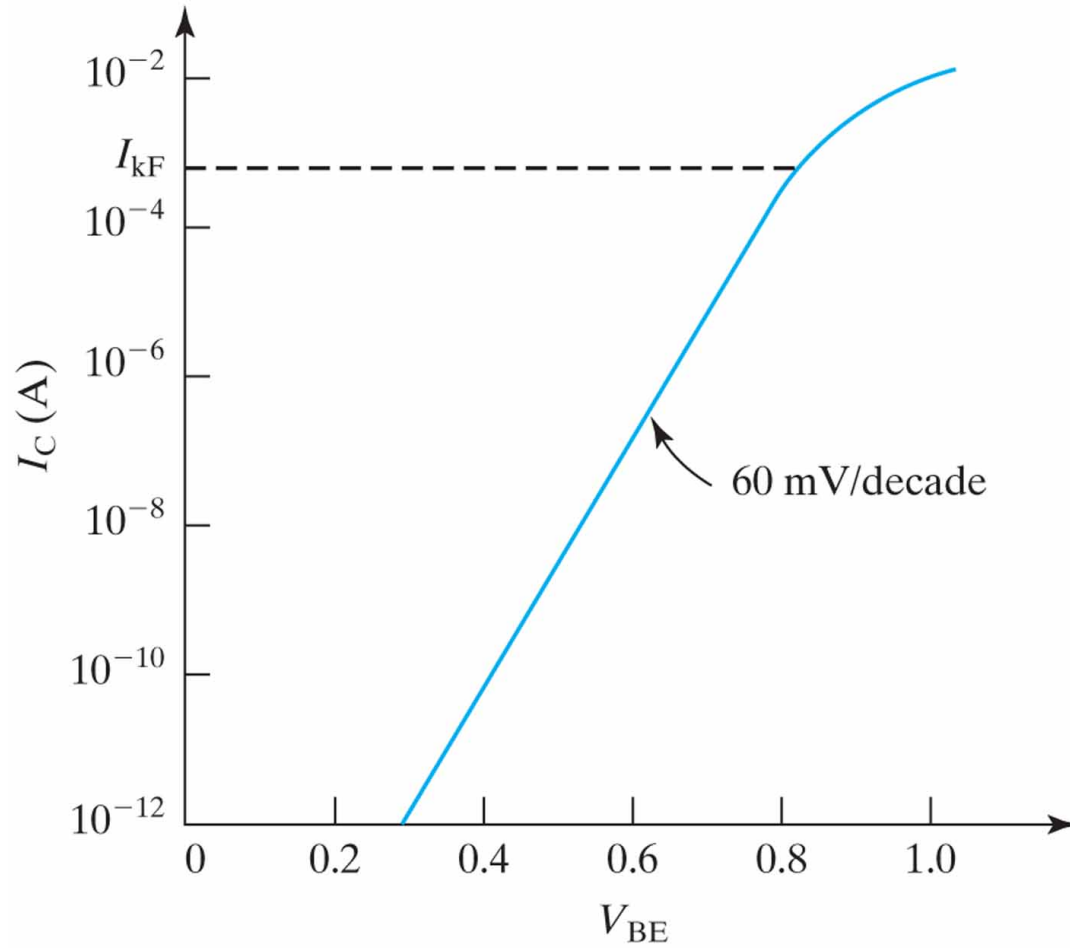
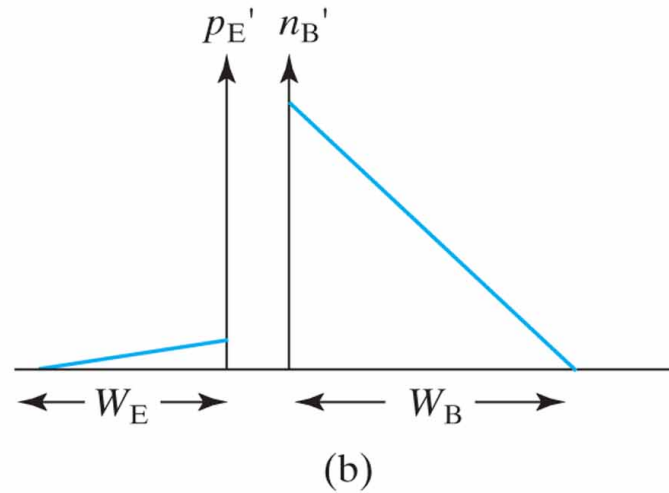
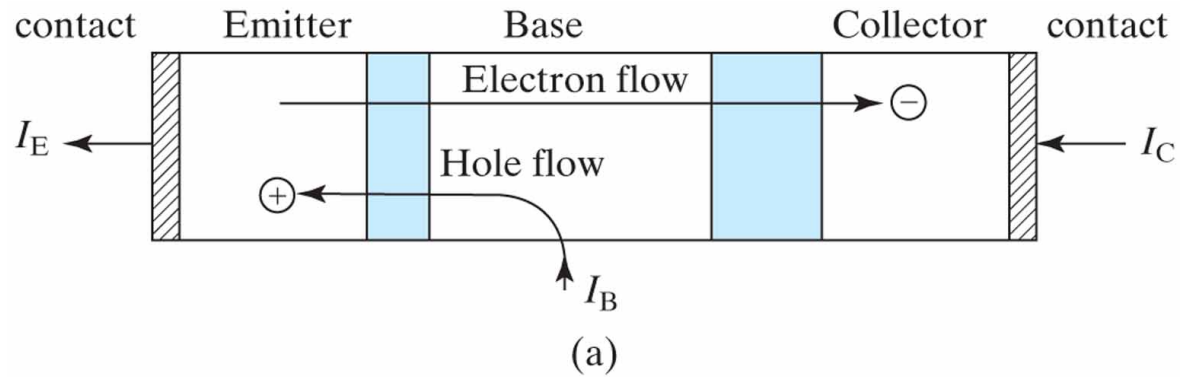


**Figure 8.6** (a) Schematic of electron and hole flow paths in BJT; (b) hole injection into emitter closely parallels electron injection into base.<sup>2</sup>



<sup>1</sup> A good metal–semiconductor ohmic contact (at the end of the emitter) is an excellent source and sink of carriers. Therefore, the excess carrier concentration is assumed to be zero.

**Figure 8.7** Schematic illustration of a poly-Si emitter, a common feature of high-performance BJTs.

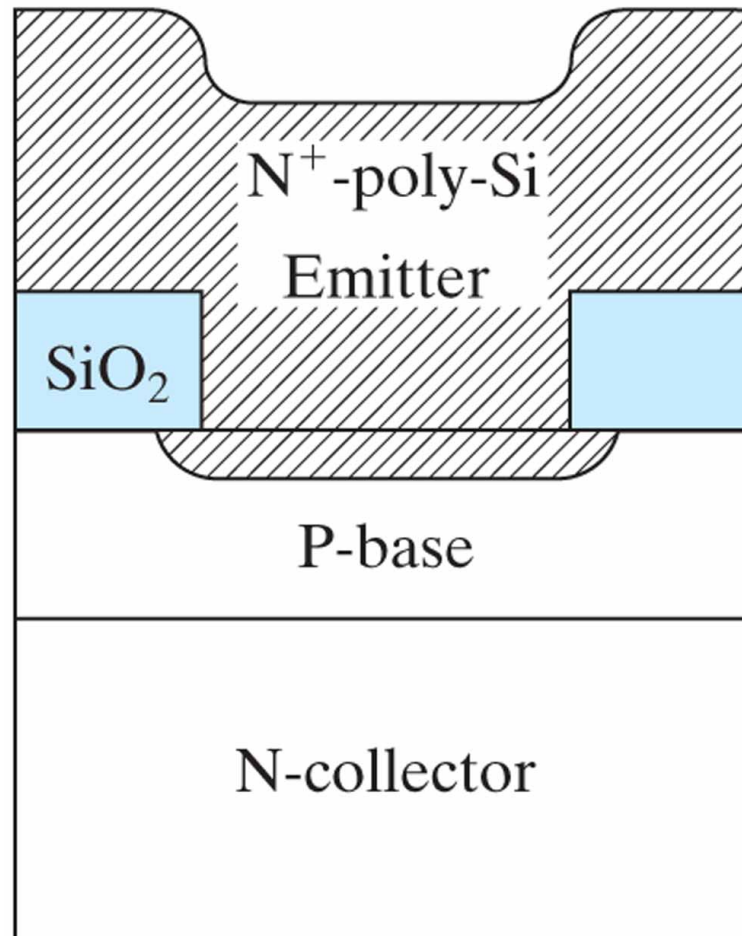


**Figure 8.8** Gummel plot of  $I_C$  and  $I_B$  indicates that  $\beta_F (= I_C/I_B)$  decreases at high and low  $I_C$ .

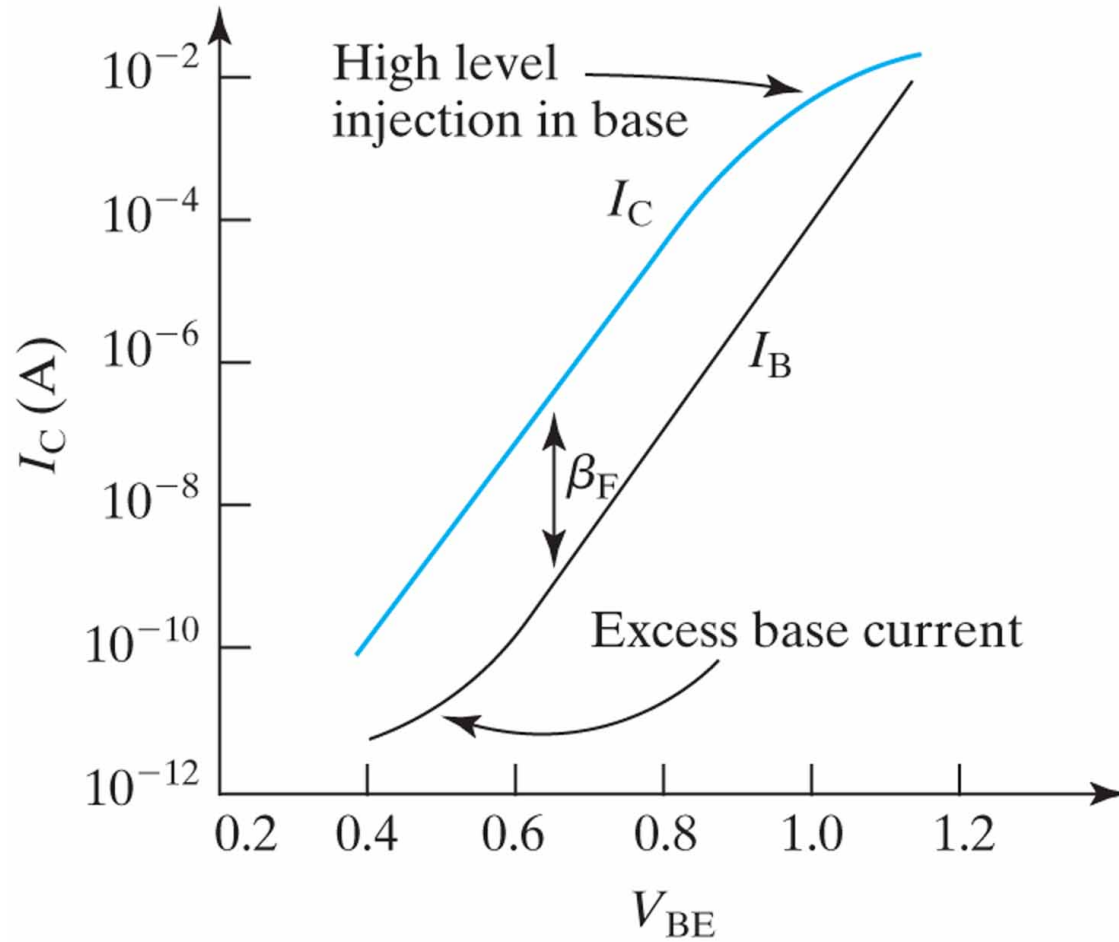


**Figure 8.9** Fall-off of current gain at high- and low-current regions.  $A_E = 0.6 \times 4.8 \mu\text{m}^2$ . From top to bottom:  $V_{BC} = 2, 1$  and  $0$  V. Symbols are data. Lines are from a BJT model for circuit simulation. (From [3].)

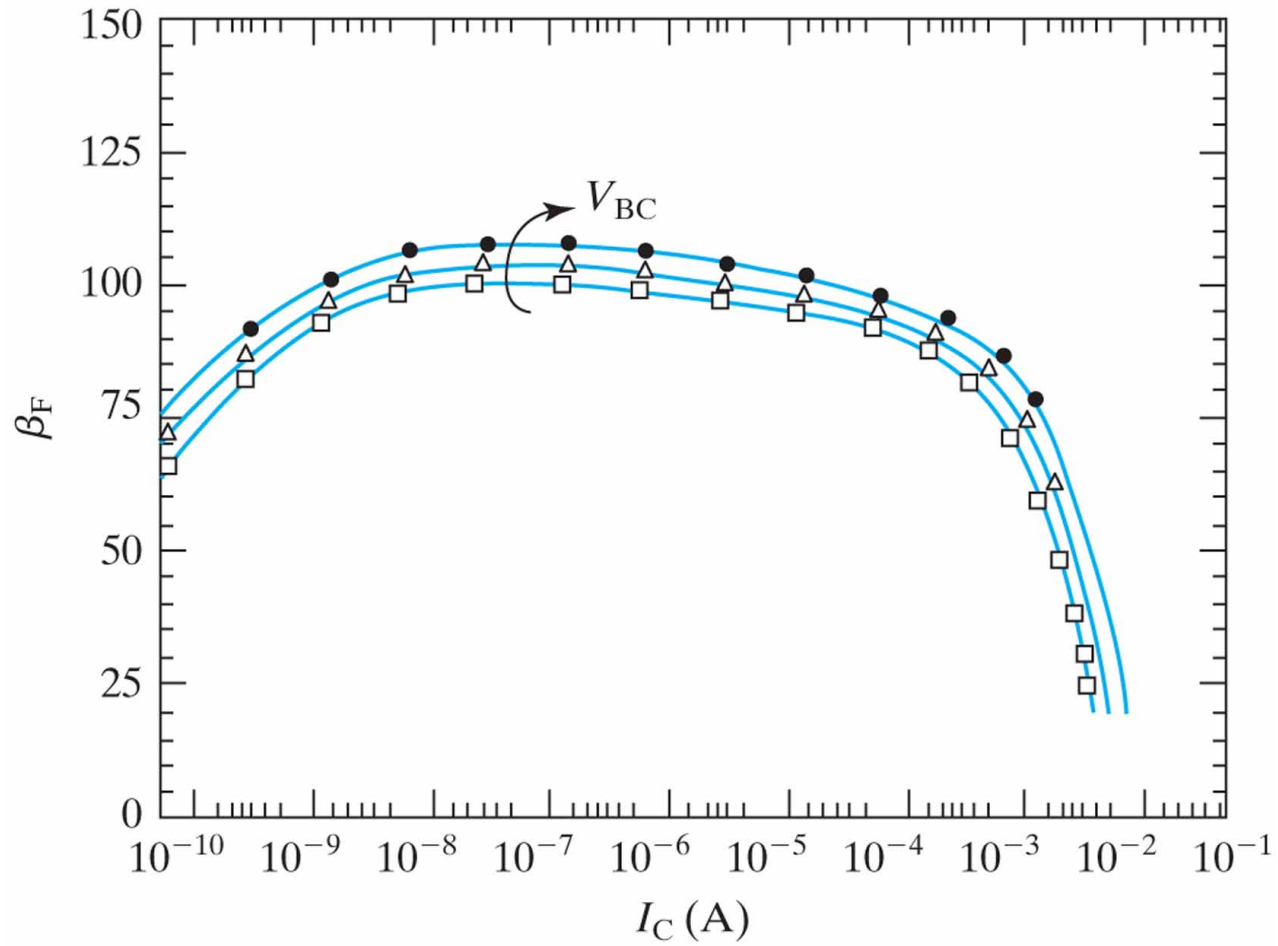
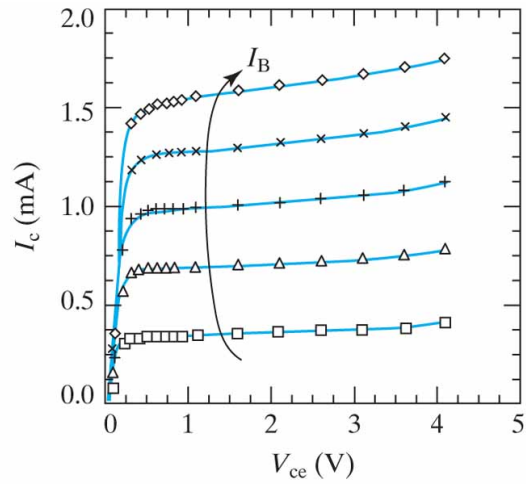
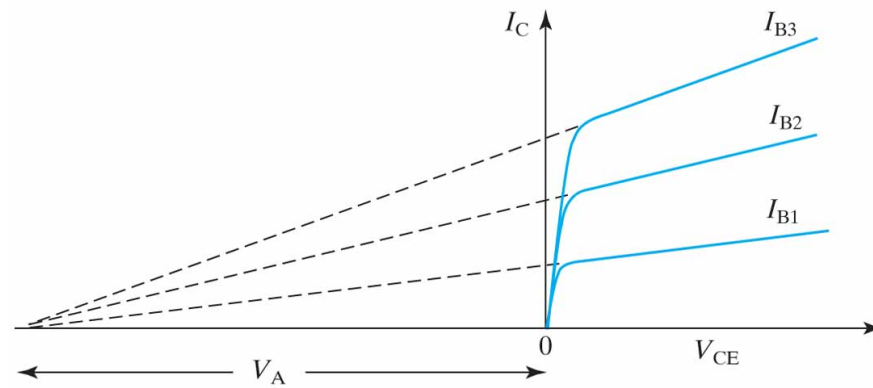


**Figure 8.10** BJT output conductance: (a) measured BJT characteristics.  $I_B = 4, 8, 12, 16,$  and  $20 \mu\text{A}$ . (From [3].); (b) schematic drawing illustrates the definition of Early voltage,  $V_A$ .



(a)



(b)

**Figure 8.11** As  $V_C$  increases, the BC depletion layer width increases and  $W_B$  decreases causing  $dn'/dx$  and  $I_C$  to increase. In reality, the depletion layer in the collector is usually much wider than that in the base.

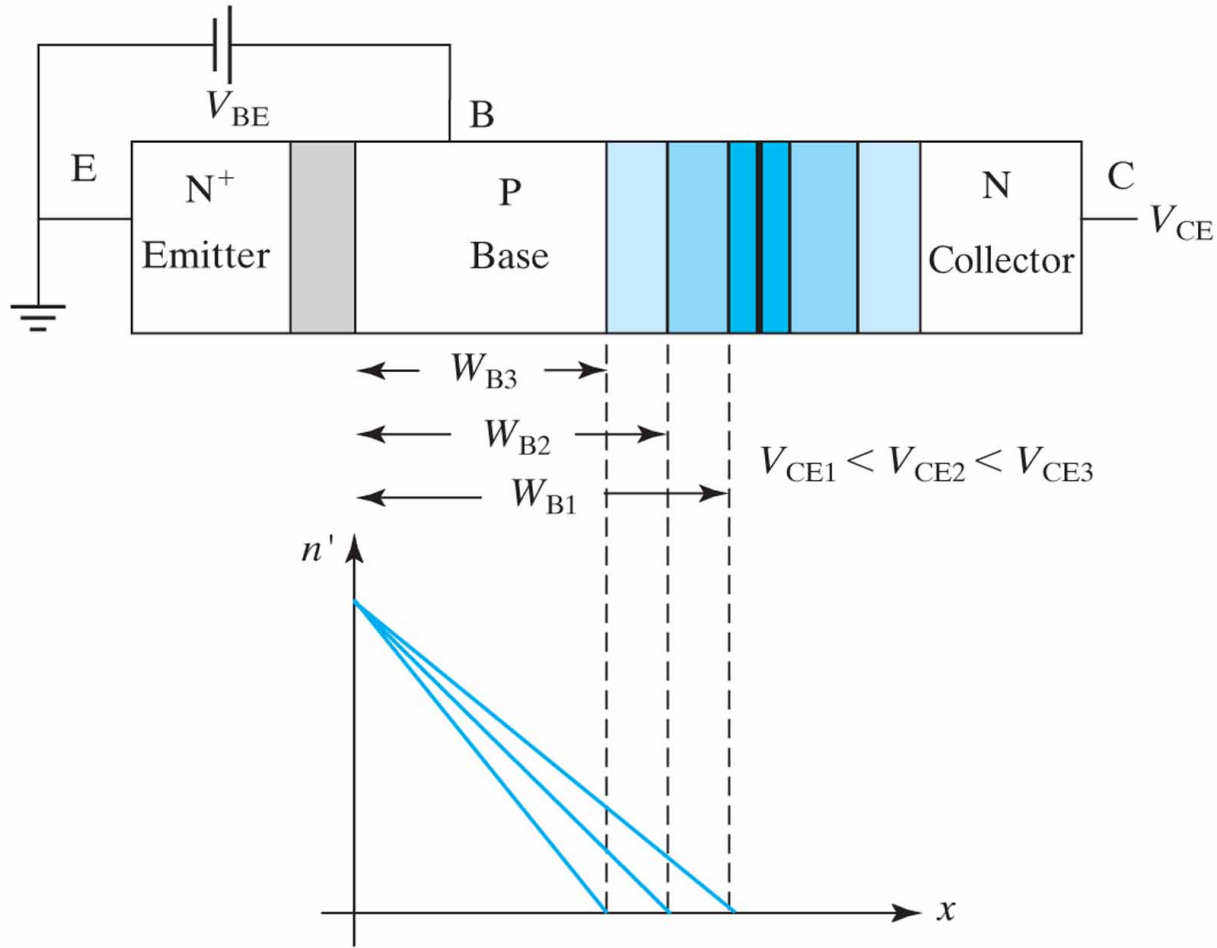


**Figure 8.12** In the saturation region,  $I_C$  drops because the collector–base junction is significantly forward biased.

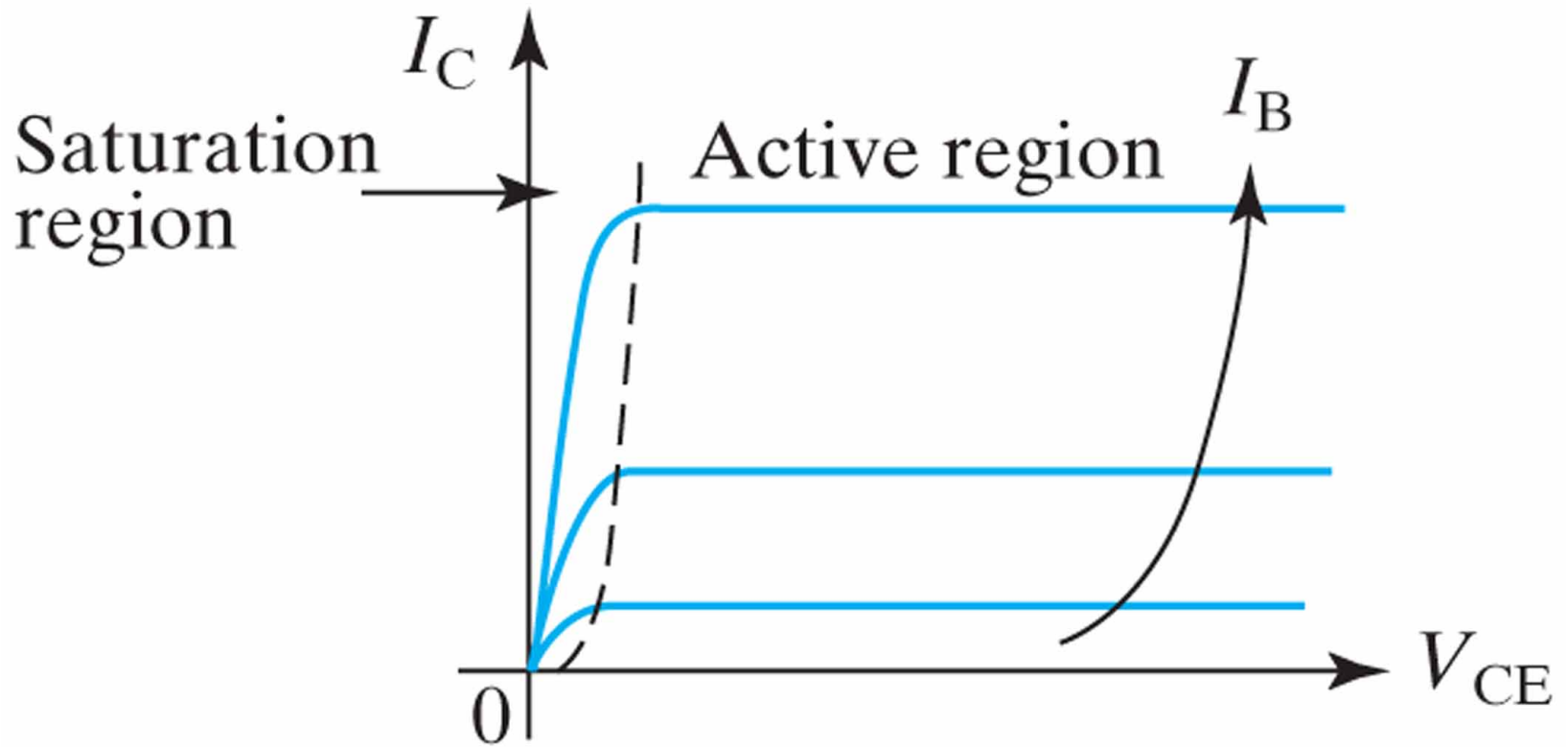
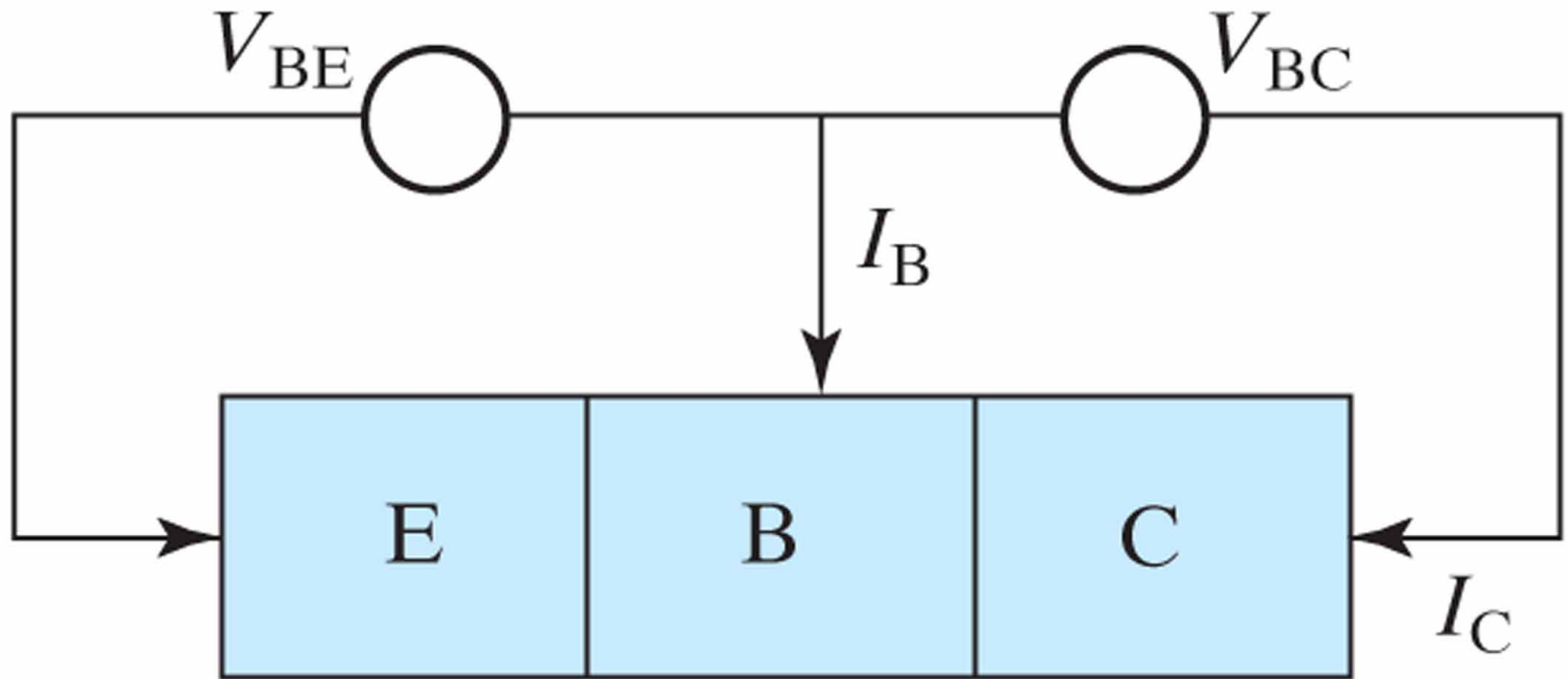
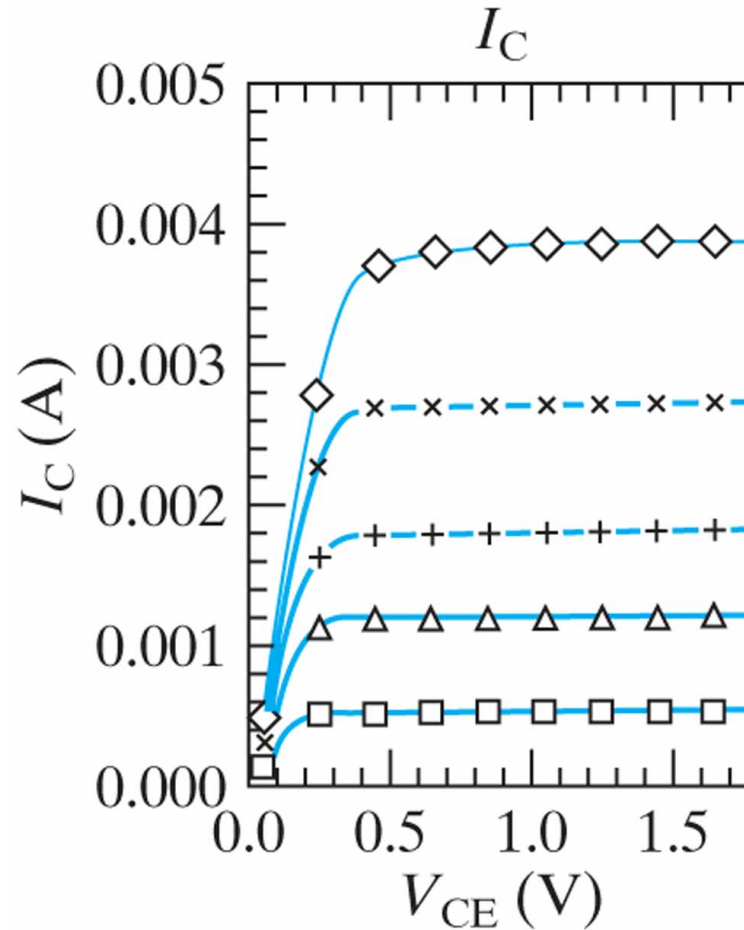


Figure 8.13  $I_C$  is driven by two voltage sources,  $V_{BE}$  and  $V_{BC}$ .



**Figure 8.14** Ebers–Moll model (line) agrees with the measured data (symbols) in both the saturation and linear regions.  $I_B = 4.3, 11, 17, 28,$  and  $43 \mu\text{A}$ . High-speed SiGe-base BJT.  $A_E = 0.25 \times 5.75 \mu\text{m}^2$ . (From [3].)



**Figure 8.15** Excess hole and electron concentrations in the base. They are equal due to charge neutrality [Eq. (2.6.2)].

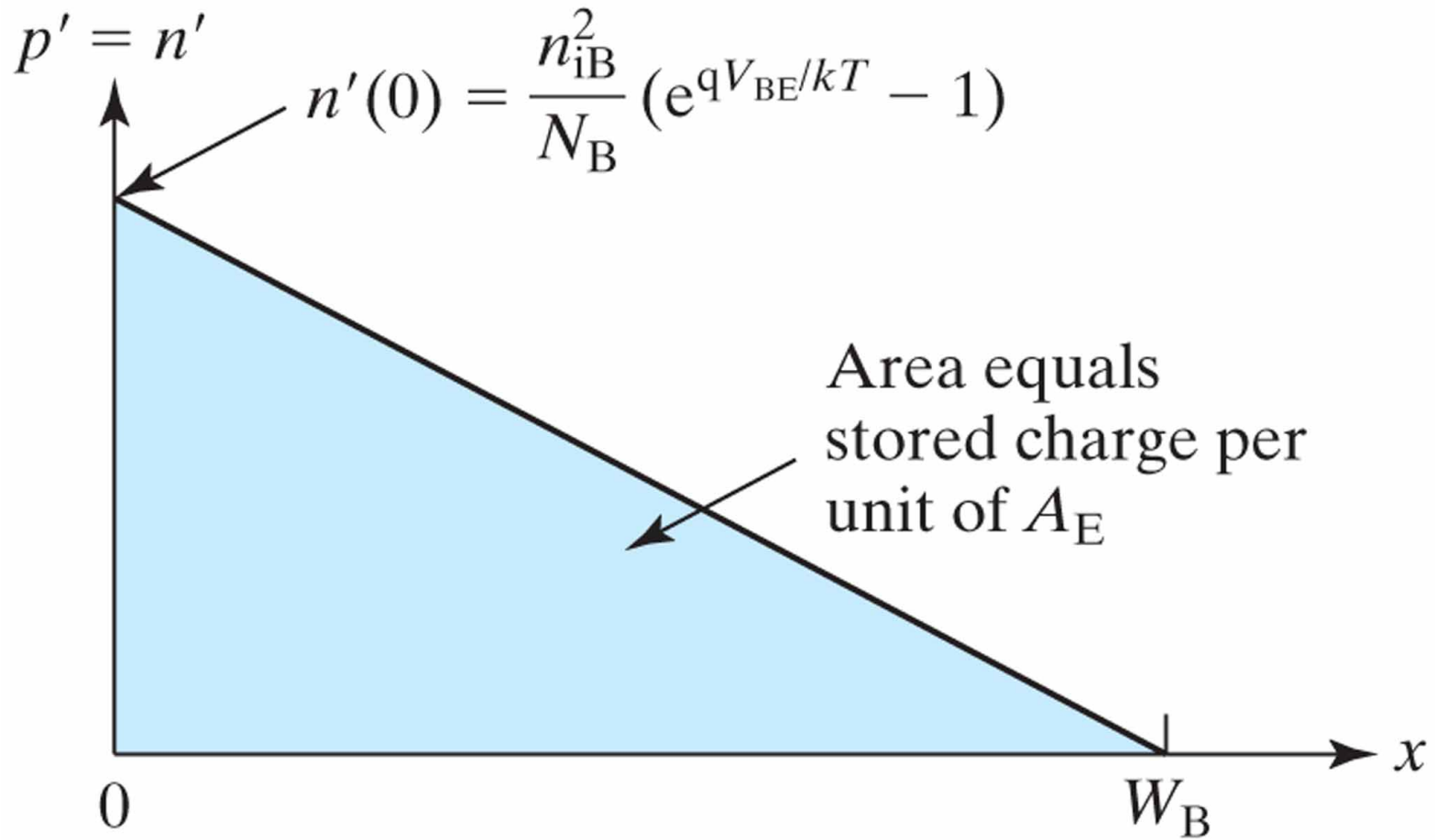




**Figure 8.17** Transit time vs.  $I_C/A_E$ . From top to bottom:  $V_{CE} = 0.5, 0.8, 1.5,$  and  $3$  V. The rise at high  $I_C$  is due to base widening (Kirk effect). (From [3].)

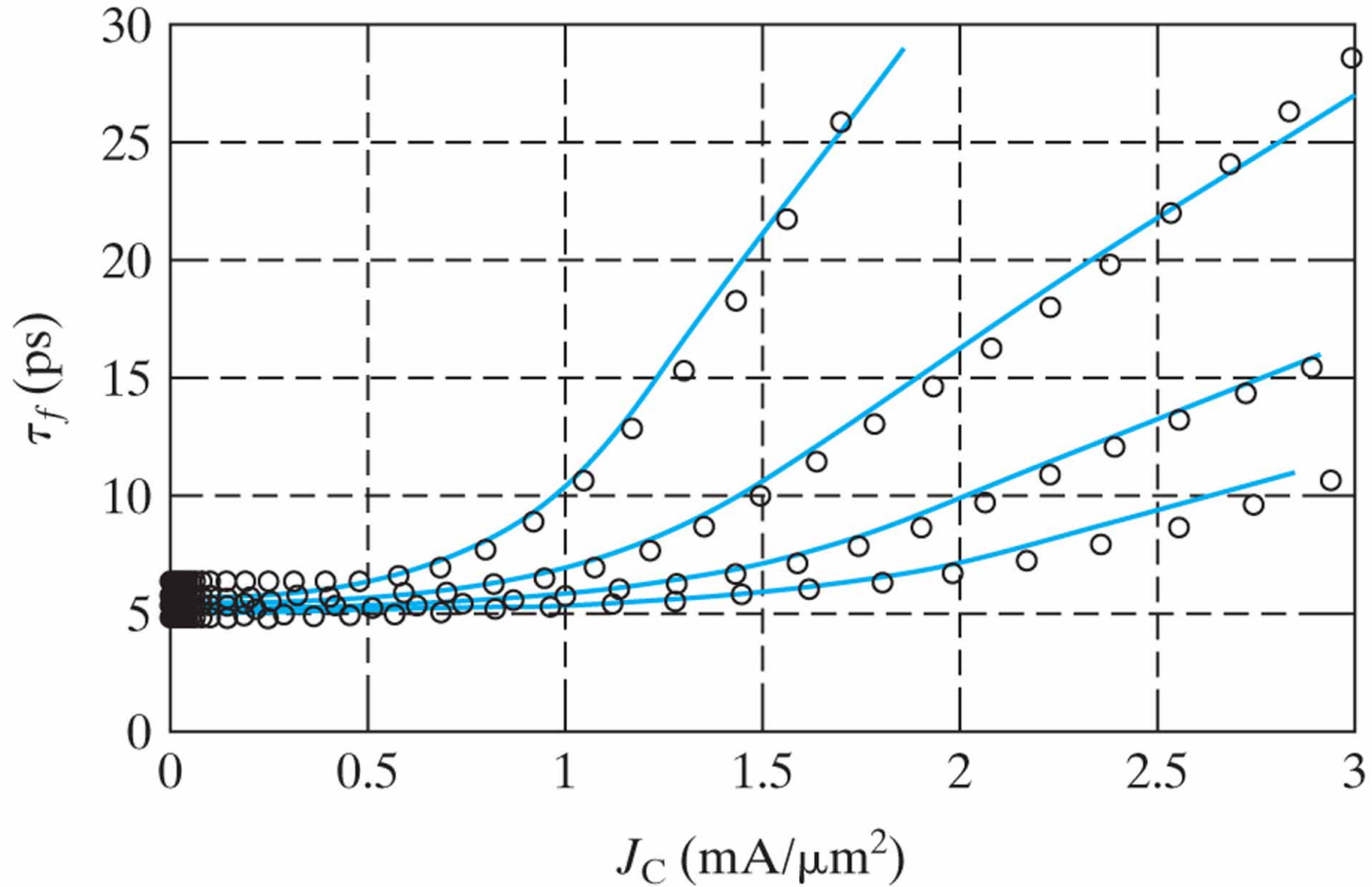


**Figure 8.18** Electric field  $\mathcal{E}(x)$ , location of the depletion layer, and base width at (a) low  $I_C$  such as  $0.1 \text{ mA}/\mu\text{m}^2$  in Fig. 8–17; (b) larger  $I_C$ ; (c) even larger  $I_C$  (such as  $1 \text{ mA}/\mu\text{m}^2$ ) and base widening is evident; and (d) very large  $I_C$  with severe base widening.

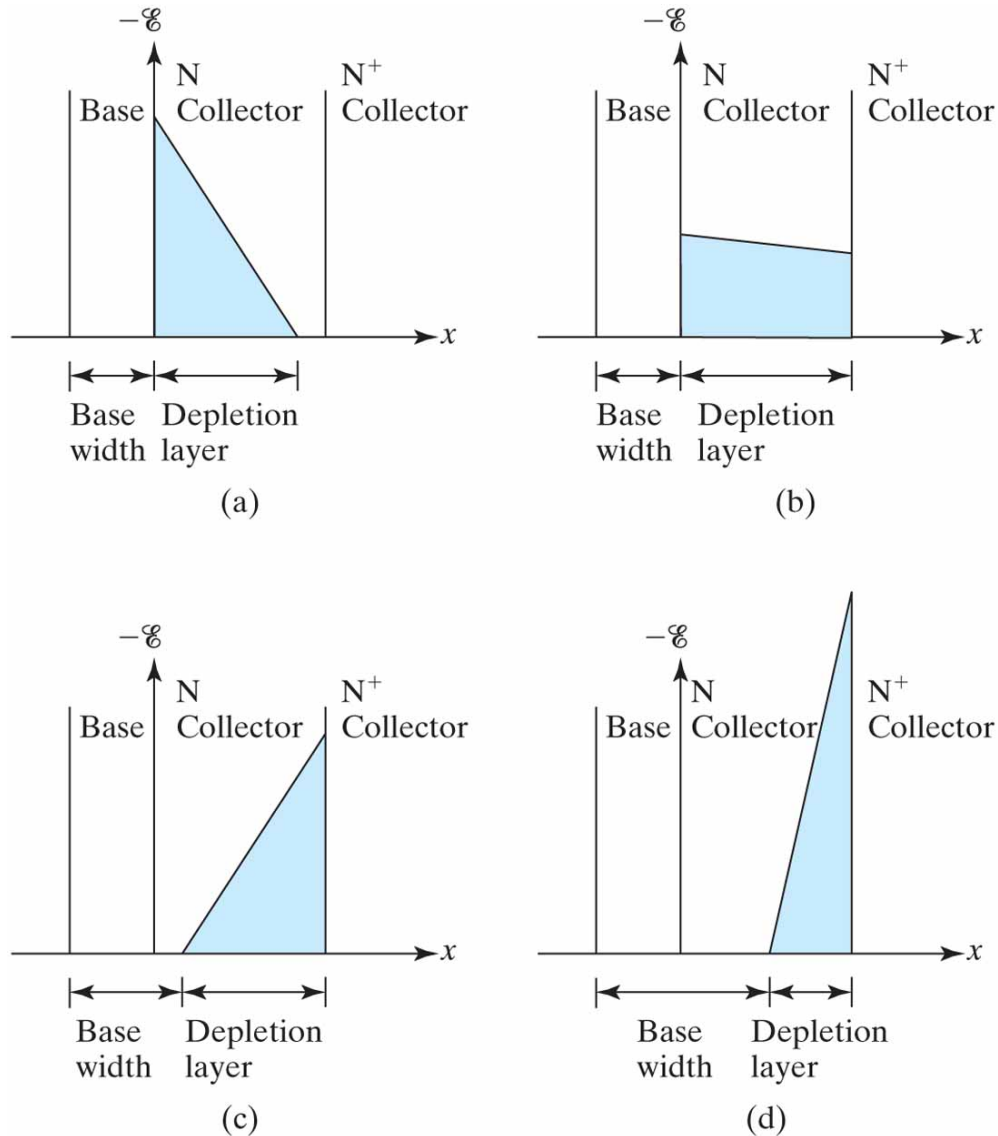


**Figure 8.19** A basic small-signal model of the BJT.

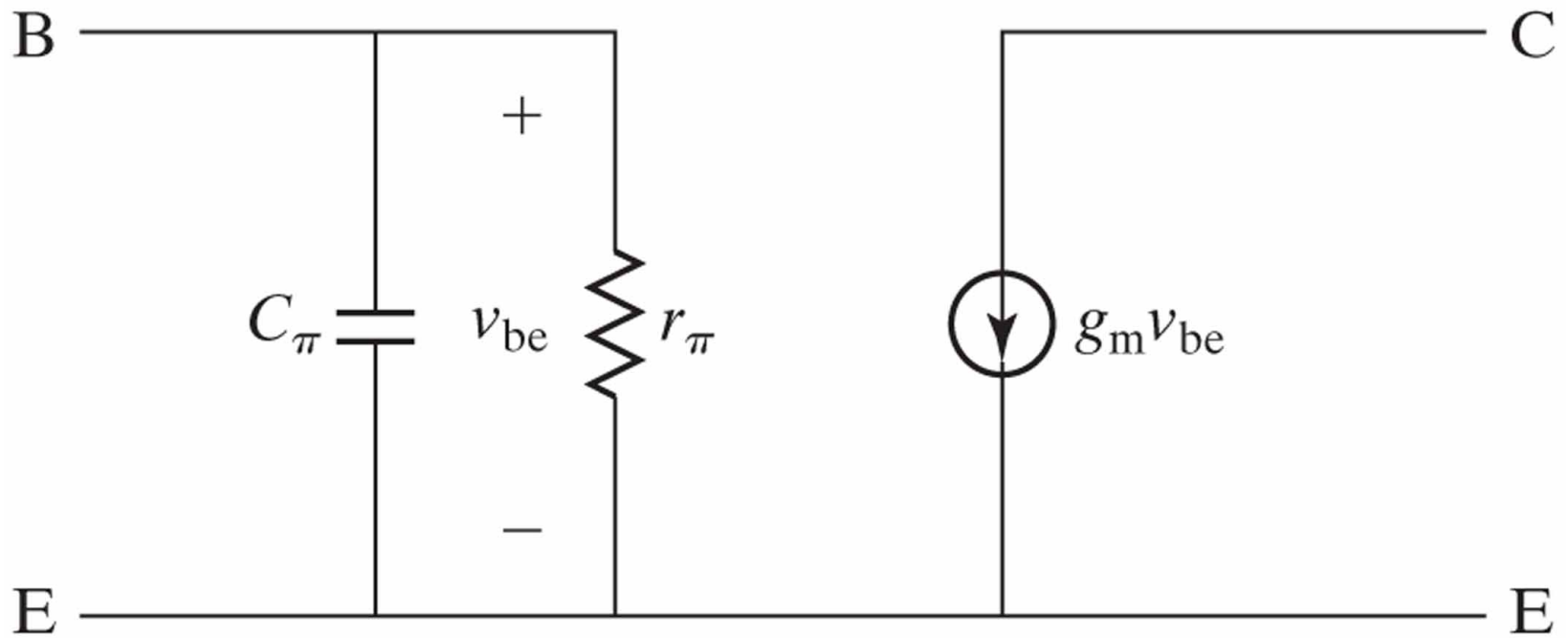


**Figure 8.20** (a) The small-signal model can be used to analyze a BJT circuit by hand; (b) a small-signal model for circuit simulation by computer.

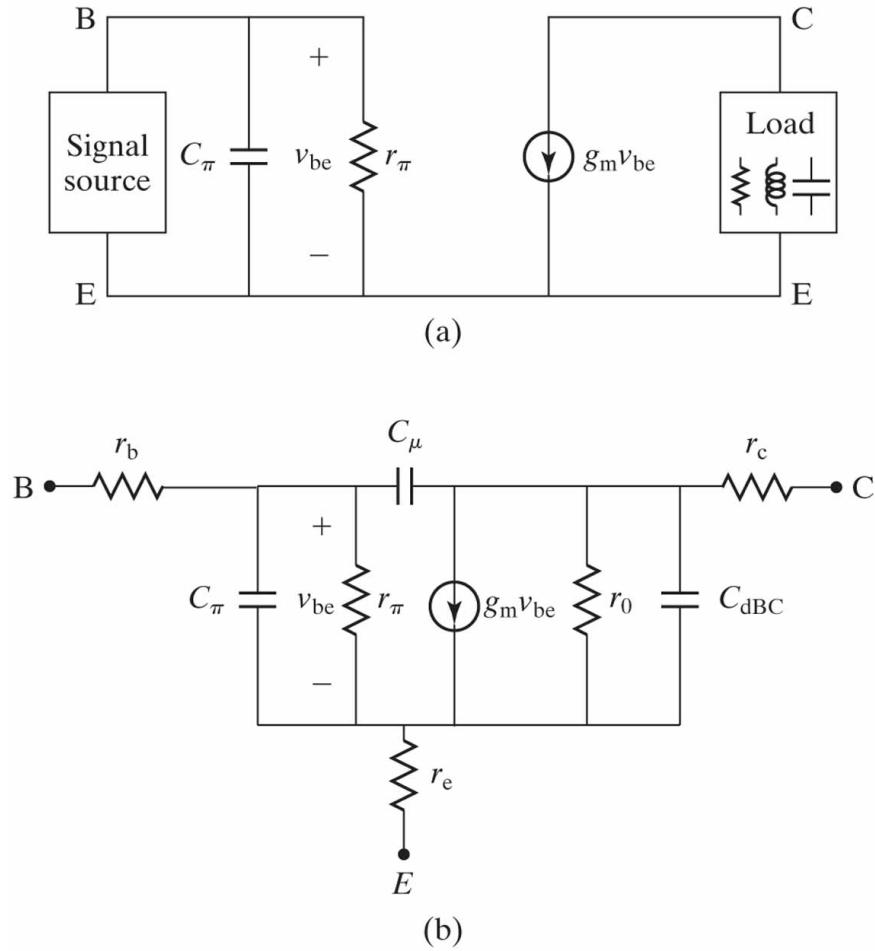


**Figure 8.21** Cutoff frequency of a SiGe bipolar transistor. A compact BJT model matches the measured  $f_T$  well. (From [6]. © 1997 IEEE.)

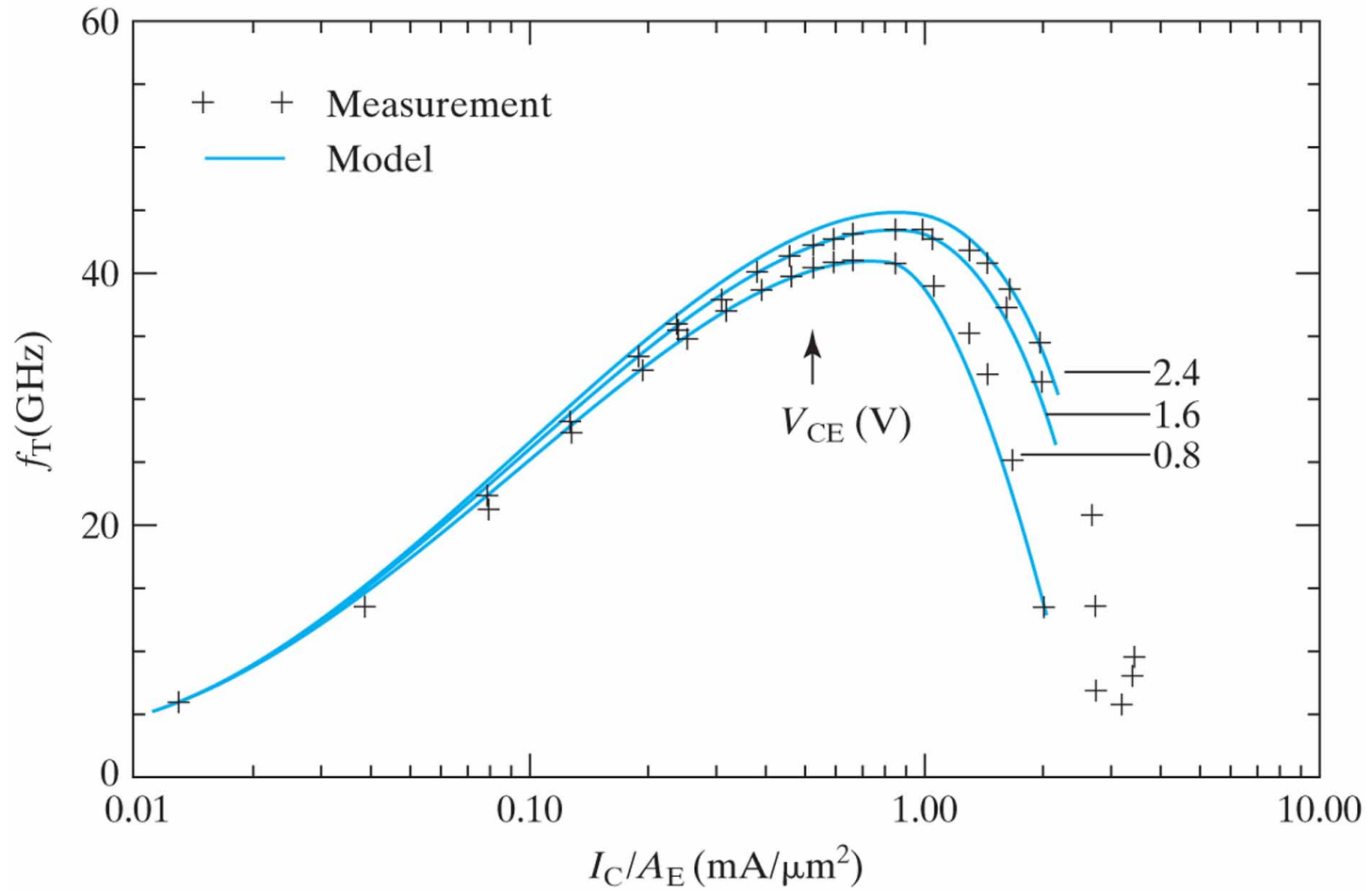


**Figure 8.22** Schematic of a BJT with poly-Si emitter, self-aligned base, and deep-trench isolation. The darker areas represent electrical insulator regions.

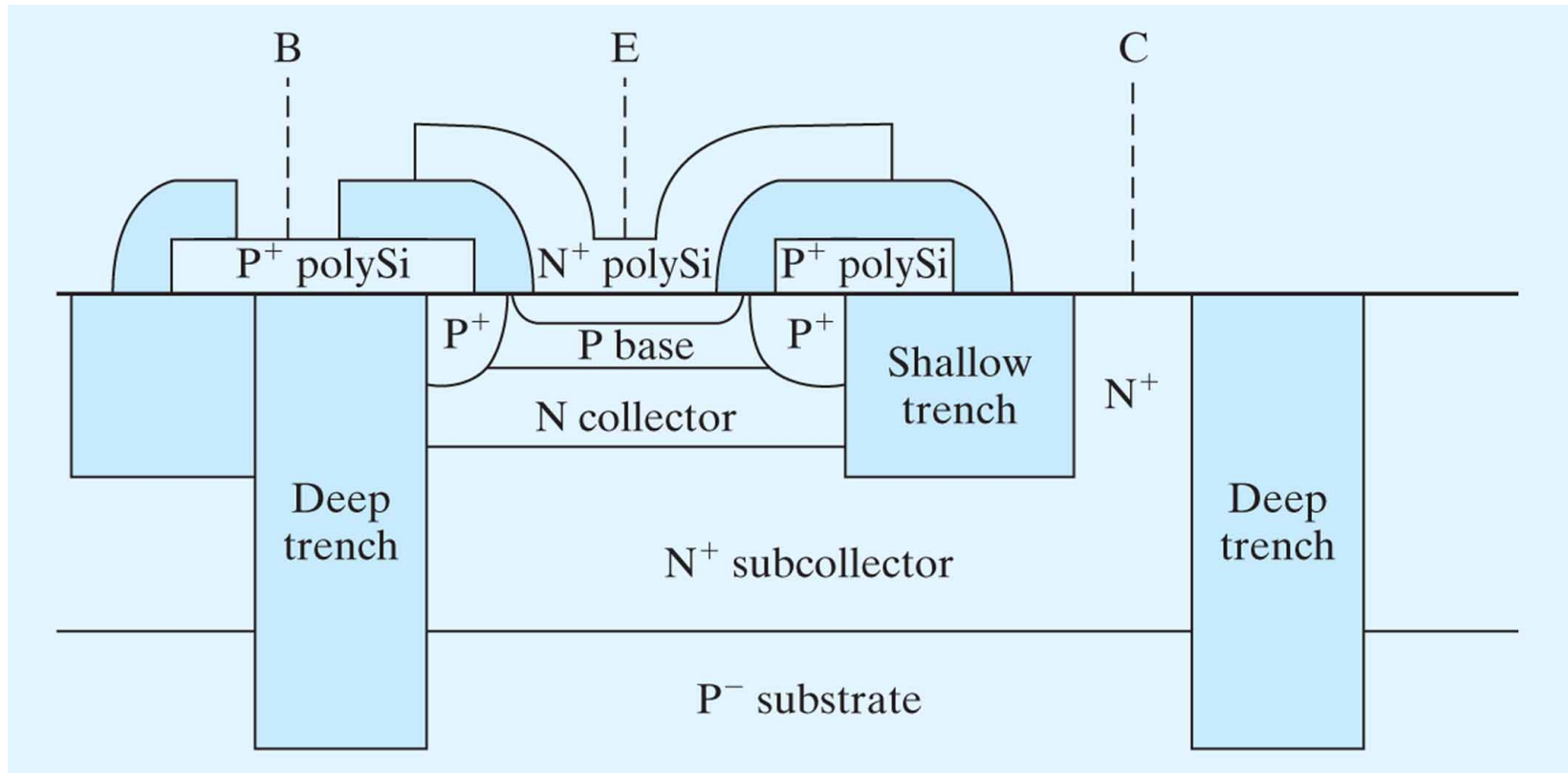


**Figure 8.23** Water analogy of the charge control model. Excess hole charge ( $Q_F$ ) rises (or falls) at the rate of supply ( $I_B$ ) minus loss ( $\propto Q_F$ ).

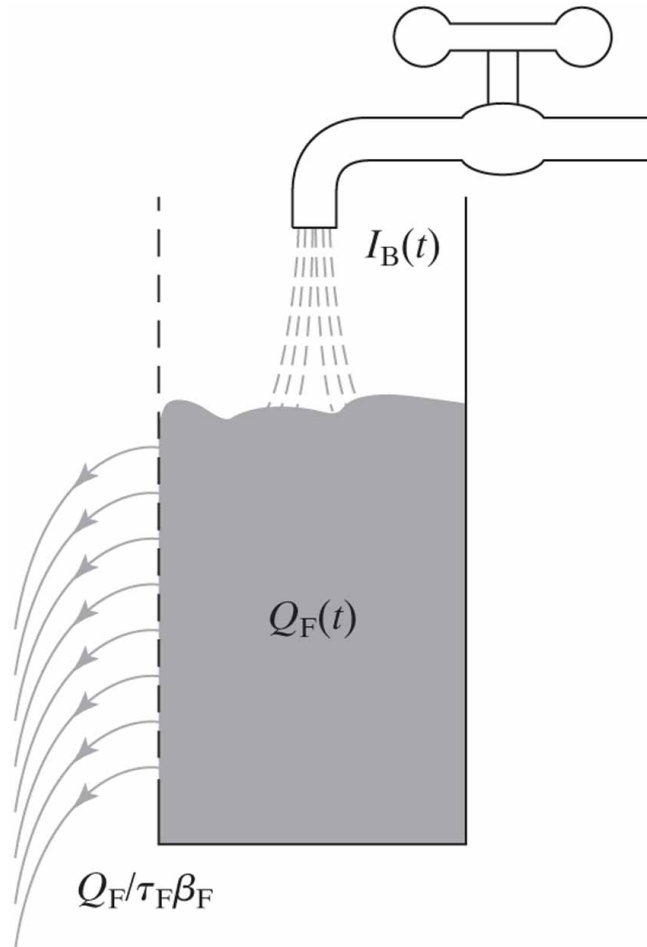


**Figure 8.24** From the given step-function  $I_B(t)$ , charge control analysis can predict  $I_C(t)$ .

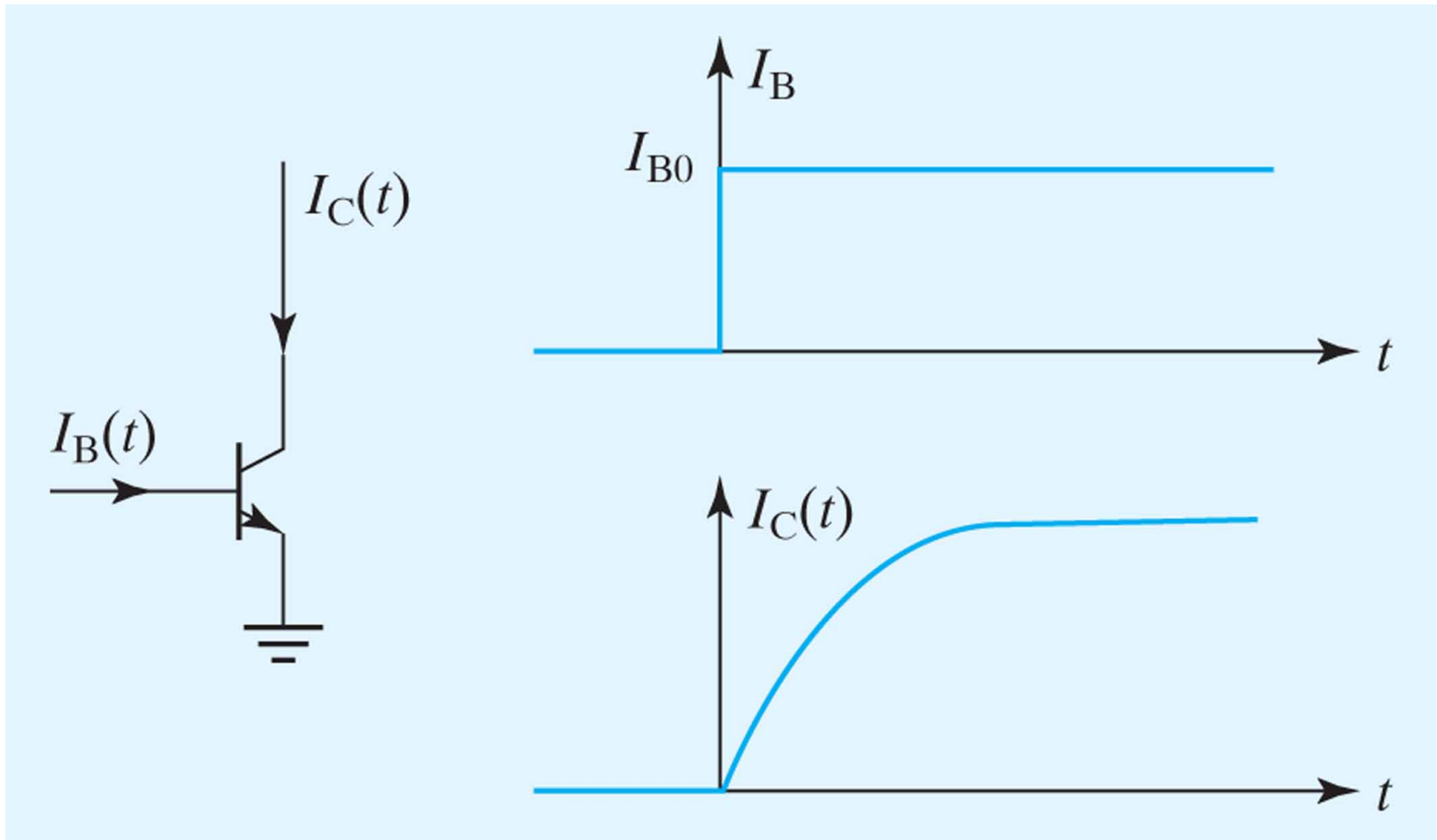


**Figure 8.25** Illustration of a BJT model used for circuit simulation.

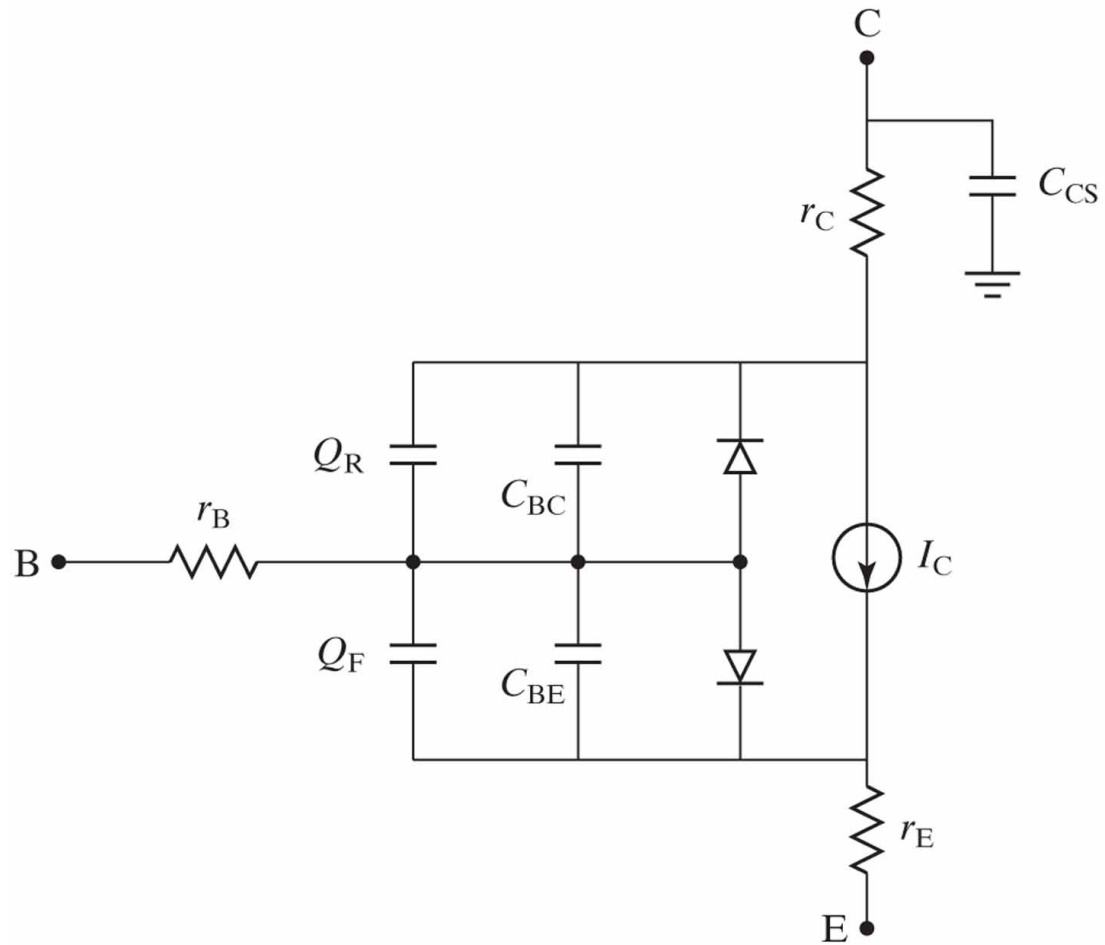


Figure 8.26

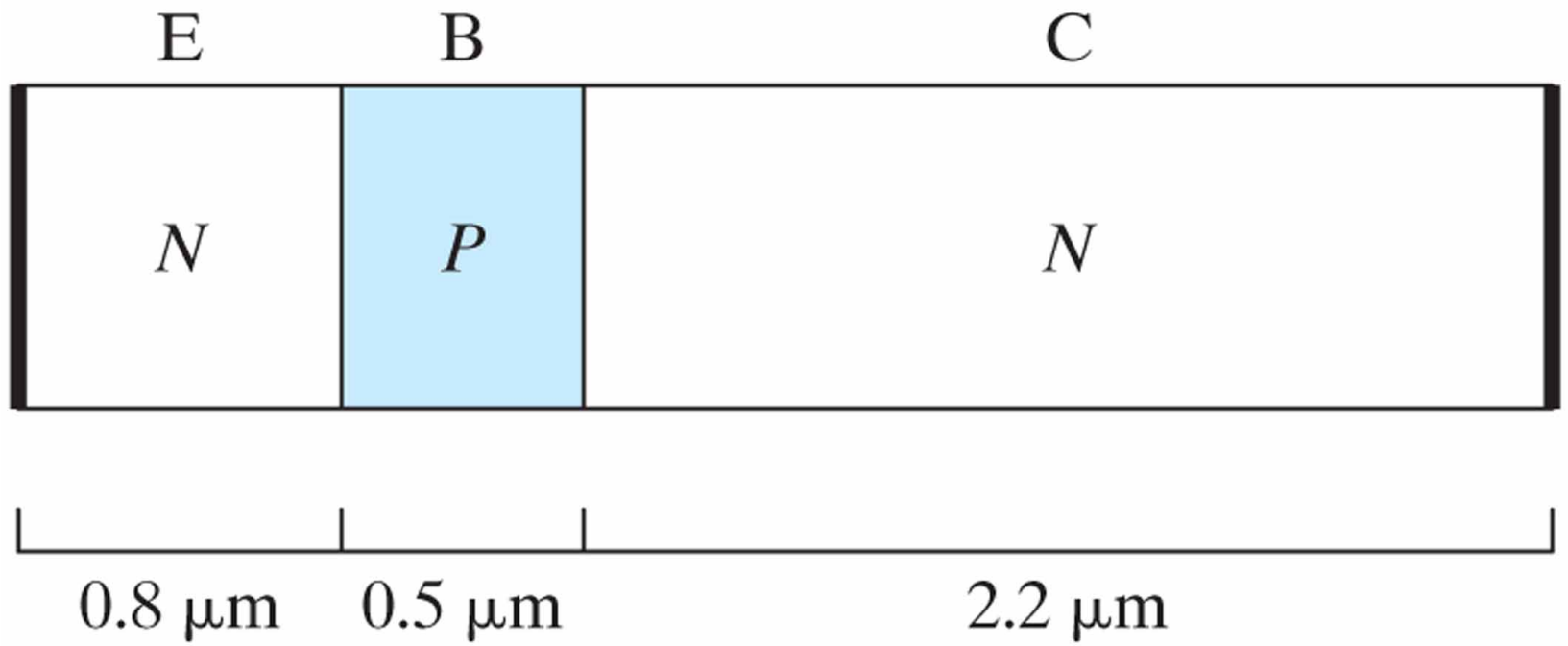


Figure 8.27

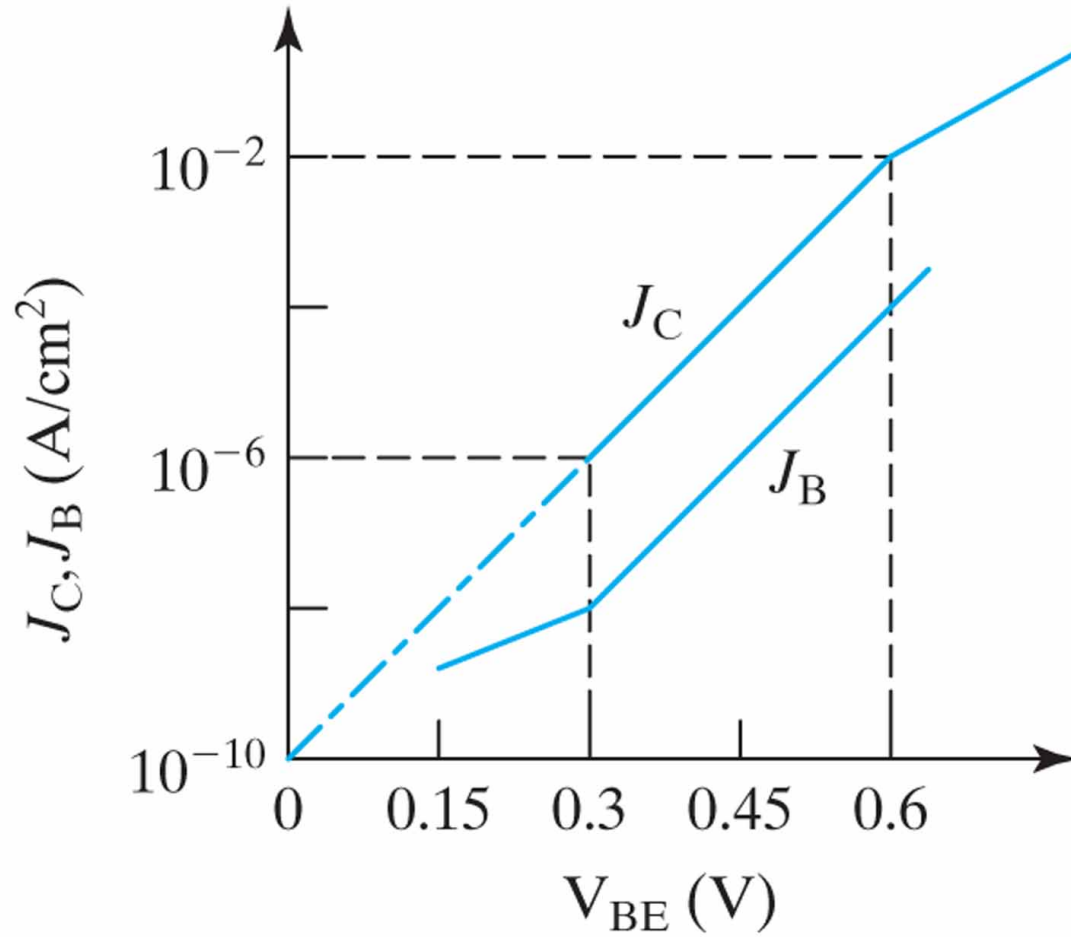


Figure 8.28

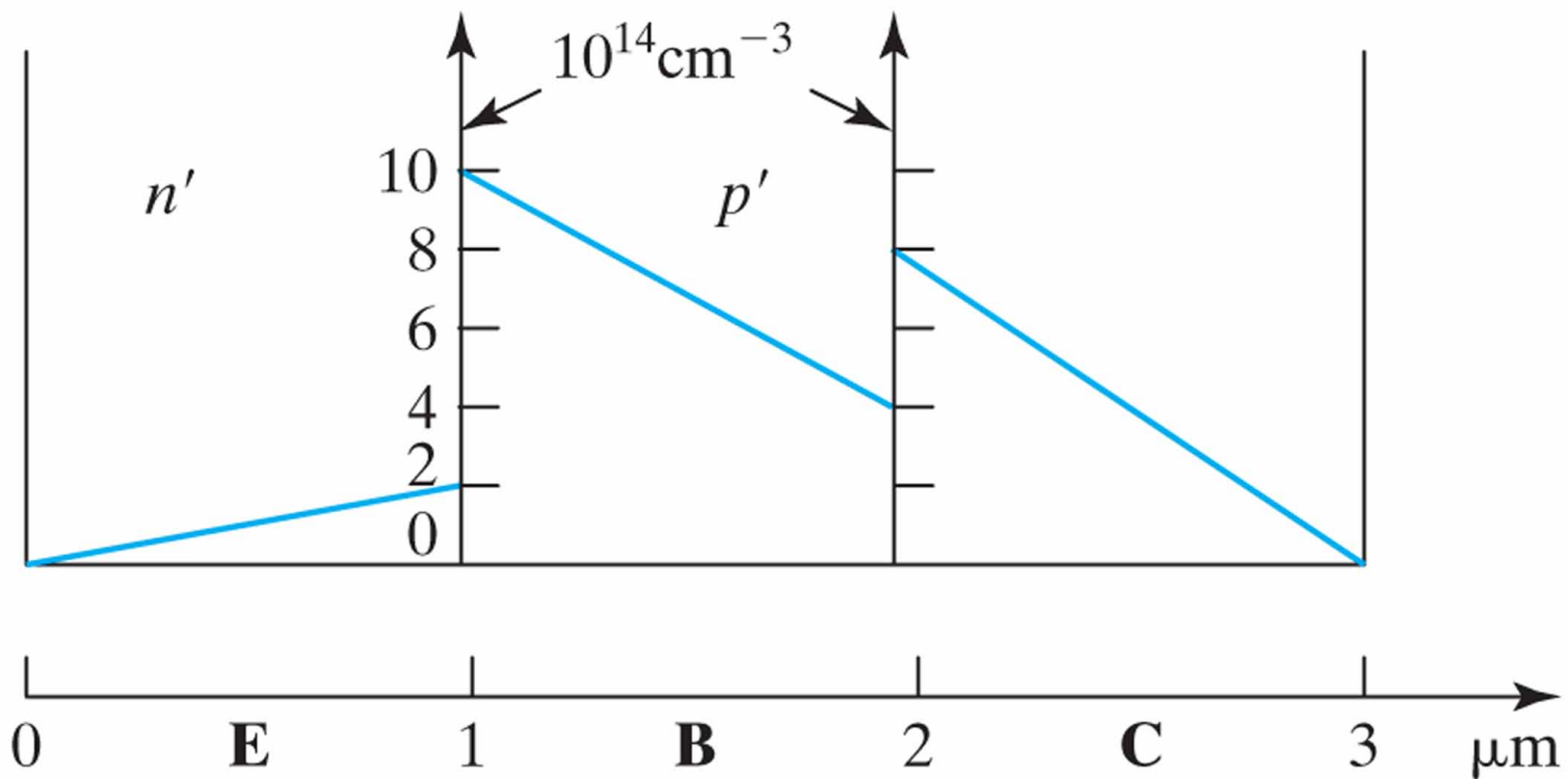


Figure 8.29

